AIP | The Journal of Chemical Physics

Complex multireference configuration interaction calculations for the K-vacancy Auger states of Nq+ (q = 2-5) ions

Yi-Geng Peng, Yong Wu, Lin-Fan Zhu, Song Bin Zhang, Jian-Guo Wang, H.-P. Liebermann, and R. J. Buenker

Citation: The Journal of Chemical Physics **144**, 054306 (2016); doi: 10.1063/1.4940733
View online: http://dx.doi.org/10.1063/1.4940733
View Table of Contents: http://scitation.aip.org/content/aip/journal/jcp/144/5?ver=pdfcov
Published by the AIP Publishing

Complex multireference configuration interaction calculations for the K-vacancy Auger states of N^{q+} (q = 2-5) ions

Yi-Geng Peng,[1,2] Yong Wu,[2,a)] Lin-Fan Zhu,[1] Song Bin Zhang,[3,4] Jian-Guo Wang,[2] H.-P. Liebermann,[5] and R. J. Buenker[5]

[1]*Department of Modern Physics, Hefei National Laboratory for Physical Sciences at Microscale, University of Science and Technology of China, Hefei, Anhui 230026, People's Republic of China*
[2]*Data Center for High Energy Density Physics, Institute of Applied Physics and Computational Mathematics, P.O. Box 8009, Beijing 100088, People's Republic of China*
[3]*School of Physics and Information Technology, Shaanxi Normal University, Xi'an 710062, China*
[4]*Max Planck Institute for the Structure and Dynamics of Matter (MPSD) and Center for Free-Electron Laser Science (CFEL), 22761 Hamburg, Germany*
[5]*Fachbereich C-Mathematik und Naturwissenschaften, BergischeUniversität Wuppertal, D-42097 Wuppertal, Germany*

(Received 15 November 2015; accepted 13 January 2016; published online 4 February 2016)

K-vacancy Auger states of N^{q+} (q = 2-5) ions are studied by using the complex multireference single- and double-excitation configuration interaction (CMRD-CI) method. The calculated resonance parameters are in good agreement with the available experimental and theoretical data. It shows that the resonance positions and widths converge quickly with the increase of the atomic basis sets in the CMRD-CI calculations; the standard atomic basis set can be employed to describe the atomic K-vacancy Auger states well. The strong correlations between the valence and core electrons play important roles in accurately determining those resonance parameters, Rydberg electrons contribute negligibly in the calculations. Note that it is the first time that the complex scaling method has been successfully applied for the B-like nitrogen. CMRD-CI is readily extended to treat the resonance states of molecules in the near future. © *2016 AIP Publishing LLC.* [http://dx.doi.org/10.1063/1.4940733]

I. INTRODUCTION

The metastable atoms and molecules play important roles in diverse fundamental physical processes, e.g., x-ray photoabsorption and photoionization (PI), resonant scattering of atoms and molecules by low-energy electrons, and dissociative attachment and recombination which occur frequently in many astrophysical objects and the outer atmosphere. With the advent of the satellite-borne x-ray detectors (Chandra and XMM-Newton) in resolution and sensitivity, the featured x-ray spectra of many elements of the astronomical objects are now accessible. The observation of nitrogen K-shell lines is useful for the hot starts, e.g., Leutenegger *et al.*[1] observed the lines of He-like and H-like nitrogen of the ejecta of η Carinae and discovered the lower limit of N/O > 9 for the nitrogen abundance, which reflects the CNO-recycle processes.

There have been a large number of studies for the K-vacancy resonance states of nitrogen ions. Shorman *et al.* and Gharaibeh *et al.*[2,3] recently measured the absolute cross sections for the K-shell PI of Li-like, Be-like, and B-like atomic nitrogen by employing the ion–photon merged-beam technique at the SOLEIL synchrotron radiation facility in Saint-Aubin, France. The PI cross section spectra are fitted into Fano profiles to extract the corresponding resonance widths. These authors also performed corresponding calculations with R-matrix, Multi-Configuration Dirac-Fock (MCDF), and screening constant by unit nuclear charge (SCUNC) methods. The K-vacancy resonance states of B-like, Be-like, and Li-like atomic nitrogen have been extensively studied in theory, including the studies of N^{4+}, N^{3+}, and N^{2+} ions by using the MCDF method by Chen and Crasemann;[4–9] the studies of N^{4+}, N^{3+}, N^{2+}, and N^{+} using the R-matrix method by Garcia *et al.*;[10] the MCDF studies of N^{3+} by Hata and Grant;[11] the complex rotational method (CRM) studies of N^{4+} and N^{3+} ions by Zhang and Yeager;[12,13] the studies of N^{4+} by Davis and Chung[14] and Wu and Xi;[15] and the studies of N^{3+} by Chung,[16] Shiu *et al.*,[17] Lin *et al.*,[18,19] Yang and Chung,[20] and Wang and Gou.[21] For the He-like atomic nitrogen ion, no experimental data are available, but it has been studied by various theoretical methods and models due to its simplicity and importance.[22–33] It should be pointed out that one of the most accurate methods has been developed recently by Derevianko *et al.*[34] to treat the atomic resonance atomic states, namely, the CI + MBPT + CRM approach, in which they combined the relativistic configuration-interaction (CI) method, the many-body perturbation theory (MBPT) method, and the CRM. The newly developed CI + MBPT + CRM approach has been applied to compute the dielectronic recombination spectrum for Li-like carbon and the high-precision results have been obtained. Unfortunately, further investigation has not been performed after that.

To the best of our knowledge, the complex coordinate methods have only been applied to treat the resonance states of He-like, Li-like, and Be-like atomic system, and thus, it

a)Authors to whom correspondence should be addressed. Email: wu_yong@iapcm.ac.cn

will be interesting to find out how effective this method is for five-electron systems. Motivated by the latest K-shell PI measurements of Shorman *et al.* and Gharaibeh *et al.*,[2,3] which can provide a good check on the reliability and accuracy of the complex coordinate method in treating the resonance states of N^{2+} ions.

The bound state methods can be conveniently "updated" to study the metastable states through the complex coordinate methods and it is different from the R-matrix and MCDF calculations in real coordinate space for which one should include all possible decay channels to get decay rate and resonance widths. In this paper, the complex multireference single- and double-excitation configuration interaction (CMRD-CI) method is employed to calculate the resonance energy and decay width of the K-vacancy nitrogen ions (N^{2+}, N^{3+}, N^{4+}, and N^{5+}). The convergence related to the size of the Gaussian basis sets has been checked, and the effects of different electron configurations on the resonance positions and widths have been studied.

CMRD-CI is a complex arithmetic version of the MRD-CI package[35–41] and can be applied for both molecular and atomic resonance calculations. In the (C)MRD-CI calculations, the molecular orbitals are optimized in the single-configurational self-consistent field (SCF) level, which is different from the multiconfigurational self-consistent field calculations.[12,13,42,43]

II. THEORETICAL METHOD

The complex scaling theorem developed by Aguilar, Balslev, and Combes[44,45] and Simon[46] in the 1970s is one of the most convenient and important ways to apply bound state methods to the study of metastable states. Within this theorem,[44–47] the electronic coordinates (r) of the Hamiltonian (H) are scaled (or "dilated") by a complex parameter η as $r \rightarrow \eta r$, where $\eta = \alpha e^{i\theta}$, $\alpha > 0$, and $\theta \in (0, 2\pi)$ are real. The bound states are real and unchanged by complex scaling, the continuum of the complex scaled Hamiltonian ($\bar{H}$) is rotated by an angle 2θ at each threshold such that the continuum states appear as complex eigenvalues of $\bar{H}$. And resonances $E = E_r - (i/2)\Gamma_r$ hidden in the continua are exposed in complex space for some suitable η, where E_r and Γ_r are the resonance energy and width, respectively. For a complete basis set, the complex eigenvalues $E(\eta)$ are unaffected when η are varied, while the continuum moves. For a finite basis set, the $E(\eta)$ trajectory in the complex plane pauses or kinks at the physical position of resonances.

Alternatively, the complex scaling method can also be implemented by scaling the basis functions as $g(r) \rightarrow g(\eta r)$, instead of the Hamiltonian.[47,49,50] The latter approach is implemented in the present work, SCF and CI calculations are performed by using the complex scaled Gaussian basis functions. Only the basis functions are scaled and all calculations are carried out on the real axis, which is computationally efficient. This approach has been justifiable in the context of exterior scaling[48] which rotates the coordinates in the basis functions rather than in the operators.

Generally, the resonances can be determined by only varying the scaling parameter θ with a big basis set. Bearing in mind that the scaling parameter α scales the absolute value of the exponents of the basis functions and helps to better describe the relaxation effect of the electron wavefunction of the vacancy state. Therefore, the resonances can be more precisely determined even with smaller basis sets by varying both the scaling parameters α and θ. In the present work, the calculations are carried out with a complex arithmetic version of MRD-CI package[35–41] (CMRD-CI) using the Table-CI algorithm.[35–37]

The CMRD-CI package has been successfully applied to treat the shape resonance and Feshbach resonance of some anionic diatomic molecules, including HCl^-, F_2^-, and N_2^-,[51–53] as well as the auto-ionization states of H_2 and HeH;[54] the details of the CMRD-CI method have been presented in these works. Here, we just emphasize some of its basic ideas which are relevant to the present application. In the complex SCF calculations, the variational principle is applied to obtain the eigenfunctions of the molecular orbital, which serve as one-electron basis functions for constructing the determinantal wavefunctions. In the CI calculation, all electrons are treated as active and the single- and double-excitations are included to construct the configuration space, and the individual selection schemes[39] specific for each reference configurations are applied for the configuration selections and the Davidson subspace method[55,56] is used for diagonalization. Finally, stationary solutions of the energy expectation value on the scaling parameter η can be found in the complex plane by varying α and θ. Note that the stationary principle is applicable for both the SCF and CI calculations. In the case of shape resonances, Ψ can be represented well by a single-configuration wavefunction, whereas for Feshbach resonances, the electron correlation effects become important and Ψ should be a multi-configurational wavefunction. In the present work, the CMRD-CI package is used to treat the vacancy states for the first time. In the calculations, the Gaussian basis set is built up from the correlation consistent polarized valence quintuple zeta, cc-pv5z basis function of Dunning for nitrogen.[57] Specifically, all the s-, p-, and d-type functions are discontracted (primitive) and scaled with a factor η, and the f-, g-, h-type functions are discarded to reduce the computations, a 14s8p4d non-contracted Gaussian-type basis is produced. In some cases, the d-type functions are also discarded and a 14s8p non-contracted Gaussian basis is employed. The Gaussian basis sets used for different resonance states are presented in Table I, along with the important decay channels and the main configurations for each resonance state. In the complex SCF calculation, the configuration of the initial resonance state is selected in the self-consistent calculation to generate the molecular orbital one-electron wavefunctions, which are subsequently employed to form the determinants and CI wavefunctions. In the complex CI calculations, the configurations of the initial resonance state and the main decay states are selected as the reference configurations. Thousands to hundreds of thousands of configurations are involved in the calculations for different resonance states. In the end, the resonances are determined by the trajectory method.[58] Generally, the position where the trajectories (both α- and θ-trajectories) turn into a "cusp" or "slowing down" serves as the resonance, which is the consequence of the fact that there is a stationary principle underlying the trajectory method and

TABLE I. Shown are the Auger states (labeled as A, B, ..., Z″) of N^{q+} (q = 2-5) ions. The employed Gaussian basis type, the dominant configurations (percentage), and the dominant decay channels for each Auger state are shown in the third, fourth, and fifth columns, respectively.

Ion	States (label)	Basis type	Dominant decay channels	Dominant configurations (percentage)
N^{5+}	$2s^2\,{}^1S$ (A)	SPD	$1s+\epsilon s$	$2s^2$ (74.9%) + $2p^2$ (23.8%)
	$2s2p\,{}^{1,3}P$ (B,C)	SPD	$1s+\epsilon p$	$2s2p$ (98.7%), $2s2p$ (99.3%)
N^{4+}	$1s2s^2\,{}^2S$ (D)	SP	$1s^2+\epsilon s$	$1s2s^2$ (87.9%) + $1s2p^2$ (10.4%)
	$1s[2s2p\,{}^{1,3}P]\,{}^2P$ (E,F)	SP	$1s^2+\epsilon p$	$1s2s2p$ (99.2%), $1s2s2p$ (99.3%)
	$1s2p^2\,{}^2D$ (G)	SPD	$1s^2+\epsilon d$	$1s2p^2$ (91.9%)
	$1s2p^2\,{}^2S$ (H)	SP	$1s^2+\epsilon s$	$1s2p^2$ (87.3%) + $1s2s^2$ (11.2%)
N^{3+}	$1s2s^22p\,{}^{1,3}P$ (I,J)	SP	$1s^22s+\epsilon p, 1s^22p+\epsilon s$	$1s2s^22p$ (91.0%), $1s2s^22p$ (90.0%)
	$1s2s2p^2\,{}^1S$ (N)	SP	$1s^22s+\epsilon s$	$1s2s2p^2$ (93.2%), $1s2s2p^2$ (92.9%)
	$1s[2s2p^2\,{}^{2,4}P]\,{}^3P$ (K,L)	SP	$1s^22p+\epsilon p$	$1s2s2p^2$ (94.5%), $1s2s2p^2$ (93.3%)
	$1s2s2p^2\,{}^1P$ (O)	SP	$1s^22p+\epsilon p$	$1s2s2p^2$ (95.6%)
	$1s2s2p^2\,{}^{1,3}D$ (M,P)	SPD	$1s^22s+\epsilon d, 1s^22p+\epsilon p$	$1s2s2p^2$ (93.8%), $1s2s2p^2$ (93.7%)
N^{2+}	$1s2s^22p^2\,{}^2S$ (V)	SP	$1s^22s^2+\epsilon s, 1s^22s2p+\epsilon p$	$1s2s^22p^2$ (89.1%) + $1s2p^4$ (5.7%)
	$1s2s^22p^2\,{}^2P$ (U)	SP	$1s^22s2p+\epsilon p$	$1s2s^22p^2$ (96.2%)
	$1s2s^22p^2\,{}^2D$ (T)	SPD	$1s^22s^2+\epsilon d, 1s^22s2p+\epsilon p$	$1s2s^22p^2$ (91.7%)
	$1s2s2p^3\,{}^2S$ (X)	SP	$1s^22p^2+\epsilon p$	$1s2s2p^3$ (95.4%)
	$1s[2s2p^3\,{}^{3,5}S]\,{}^4S$ (S,W)	SP	$1s^22p^2+\epsilon p$	$1s2s2p^3$ (97.1%), $1s2s2p^3$ (96.6%),
	$1s2s2p^3\,{}^4P$ (R)	SPD	$1s^22p^2+\epsilon p, 1s^22s2p+\epsilon s, 1s^22s^2+\epsilon p, 1s^22s2p+\epsilon d$	$1s2s2p^3$ (94.4%)
	$1s[2s2p^3\,{}^{1,3}P]\,{}^2P$ (Z,Y)	SPD	$1s^22p^2+\epsilon p, 1s^22s2p+\epsilon s, 1s^22s^2+\epsilon p, 1s^22s2p+\epsilon d$	$1s2s2p^3$ (95.3%), $1s2s2p^3$ (93.2%)
	$1s2s2p^3\,{}^4D$ (Q)	SPD	$1s^22s2p+\epsilon d, 1s^22p^2+\epsilon p 1s2s2p^3$ (94.6%)	
	$1s[2s2p^3\,{}^{1,3}D]\,{}^2D$ (Z″,Z′)	SPD	$1s^22s2p+\epsilon d, 1s^22p^2+\epsilon p$	$1s2s2p^3$ (93.1%), $1s2s2p^3$ (92.5%)

that the resonance root satisfies a complex viral theorem.[12,13] In the present work, the scaling factors α and θ have been varied in the ranges of 0.6–2.0 and 0°–30°, respectively.

III. RESULTS

CMRD-CI is employed to compute the resonance positions and widths for a series of K-vacancy Auger states of nitrogen ions, including the $2s^2\,{}^1S$ and $2s2p\,{}^{1,3}P$ states of N^{5+}, $1s[2s2p\,{}^{1,3}P]^2P$, $1s2s^2\,{}^2S$, $1s2p^2$ [^2S, ^2D] states of N^{4+}; $1s2s22p\,{}^{1,3}P$, $1s2s2p^2$ [$^{1,3}S$, $^{1,3}P\,{}^{1,3}D$] states of N^{3+}; and $1s2s^22p^2$ [^2S, ^2P, ^2D], $1s2s2p^3$ [$^{2,4}S$, $^{2,4}P$, $^{2,4}D$] states of N^{2+}. These 28 Auger states are labeled as A, B, C, ..., Z, Z′, Z″, respectively, as shown in the first two columns of Table I. The third column shows the type of Gaussian functions employed in the calculations, while the fourth and fifth columns show the dominant configurations and the dominant decay channels for each Auger state, respectively. The configurations contributing to the Auger state by more than 1% are listed, the residual correlations are considered by including the single- and double-excitation configurations based on the dominant configurations.

Note that the atomic basis functions for each resonance state are chosen by considering the dominant decay channels and the dominant configurations of the specific state, as shown in Table I. In principle, inclusion of the basis functions with higher symmetric functions (f- and g-type functions) will improve the results; however, the improvements are minor in the present work, since the employed basis functions can describe the dominant configurations and decay channels well.

The convergence of the calculations on the basis set size has been checked first. Auger states $1s2s^2\,{}^2S$ and $1s[2s2p\,{}^3P]\,{}^2P$ of N^{4+} are chosen as examples and the calculated absolute resonance energies are shown in Table II, where the basis sets 12s6p, 14s8p, and 16s10p, modified from cc-pVqZ, cc-pV5Z, and cc-pV6Z of nitrogen,[57] respectively, have been applied. As Table II shows, the results (both real and imaginary parts) converge quickly with the increase of the size of the Gaussian basis set. Polarization functions are not important in describing the K-vacancy resonance states, since the polarization functions are designed to treat the wavefunction distortion effects of the outer shell electrons of the atom or molecule.

In the calculations, the reference configuration space employed in the CI calculations consists of the dominant configurations of the initial resonance state and those of the corresponding decay channels. After determining the resonance energies by CMRD-CI, the resonance parameters can be determined by subtracting the ground state energy of the system, which needs to be calculated separately.

The calculated resonance parameters of states A, B, and C of N^{5+} are presented in Table III, together with other available theoretical calculations. Gning *et al.*[22] and Ho

TABLE II. The absolute (complex) energies (a.u.) of resonance states $1s2s^2\,{}^2S$ and $1s[2s2p\,{}^3P]\,{}^2P$ with three different basis sets. 12s6p, 14s8p, and 16s10p are initially modified from cc-pVqZ, cc-pV5Z, and cc-pV6Z of N atom, respectively (see the text for details).

Basis set	$1s2s^2\,{}^2S$	$1s[2s2p\,{}^3P]\,{}^2P$
12s6p	(−33.2757,−0.003 24)	(−32.8847,−0.000 436)
14s8p	(−33.2786,−0.002 85)	(−32.8861,−0.000 346)
16s10p	(−33.2771,−0.003 00)	(−32.8864,−0.000 253)

TABLE III. Auger resonance positions (eV) and widths (meV) of N^{5+} ion relative to the ground state $1s^2\ ^1S$ of N^{5+} with the same basis sets.

	A: $2s^2\ ^1S$		B: $2s2p\ ^1P$		C: $2s2p\ ^3P$	
Result	Energy	Width	Energy	Width	Energy	Width
[a]	310.6341	197.15	299.1747	101.64	308.7787	9.66
[b]	310.6359	193.61	298.6473	96.06	339.4653	8.98
[c]	310.6375	193.21	299.3310	96.19	308.7897	8.84
[d]			299.3519		308.7912	
[e]			299.3121	96.06	308.8297	8.98
[f]			299.3306		308.7893	
[g]	312.1449		301.9445			
[h]	310.0869		299.4169		304.3616	
[i]	310.6356					
[j]				96.60		8.84

[a]Present work.
[b]Gning *et al.*[22]
[c]Ho.[25]
[d]Drake and Dalgarno.[26]
[e]Seminario and Sanders:[27] Calculations using the Z-dependent perturbation theory with Feshbach projection.
[f]Seminario and Sanders:[27] Calculations using the Z-dependent perturbation theory without Feshbach projection.
[g]Biaye *et al.*[28,29]
[h]Sakho *et al.*[30]
[i]Konta *et al.*[31]
[j]Manning and Sanders *et al.*[32]

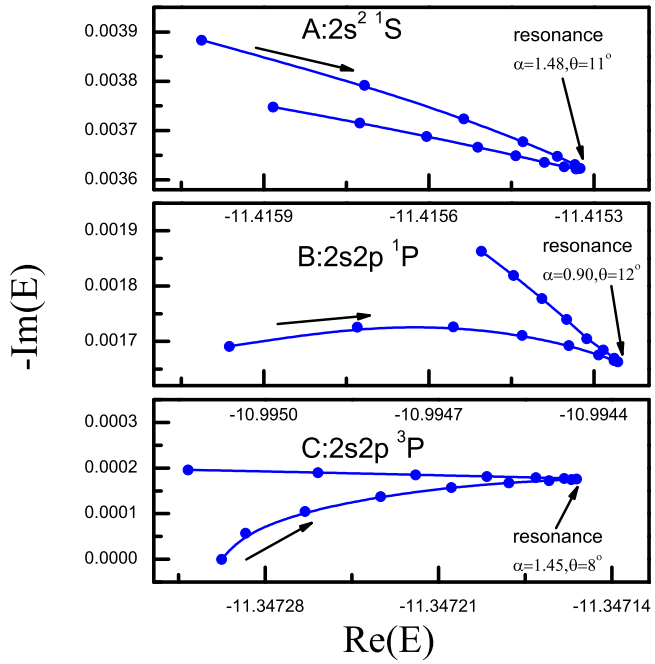

FIG. 1. θ trajectory for Auger states A, B, and C of N^{5+}, α are 1.48, 0.90, and 1.45, respectively. The step length is 1°. The calculated ground energy of N^{5+} ($1s^2\ ^1S$) is −44.7764 a.u. with basis set 14s8p4d.

et al.[25] calculated these resonance states by using the variation and complex rotation method. Seminario and Sanders[27] computed the $2s2p\ ^{1,3}P$ by using the Feshbach projection method within the framework of Z-dependent perturbation theory. Manning and Sanders[32] calculated the Auger widths by using Z-dependent perturbation theory and the complex rotation method. As shown in Table III, the present resonance parameters (positions and widths) for all the states are in excellent agreement with other calculations. The absolute differences for the widths and positions are generally within a few meV and 0.5 eV, corresponding to relative differences of less than 10% and 0.3%, respectively. Note that the calculated positions by Biaye *et al.*[28,29] differ from those of the present and others by about 2 eV. The trajectories of how to determine the resonances are also presented in Fig. 1. Generally, α- and θ-trajectories are employed alternatively, and the "cusp" or "slowing down" found in the previous trajectory will be served as initial scaling parameters for the next trajectory, resonance locates at exactly the position where "cusp" or "slowing down" overlaps for both α- and θ-trajectories. Resonances are clearly revealed in Fig. 1, showing the last θ-trajectories for states A, B, and C.

Table IV shows the present and available results of Auger states D, E, F, G, and H of N^{4+}. The last θ-trajectories and the resonances are presented in Fig. 2. The available experiment[2] was done on the SOLEIL synchrotron radiation facility,

TABLE IV. Auger resonance positions (eV) and widths (meV) of N^{4+} ion relative to the ground state $1s^22s\ ^2S$ of N^{4+} with the same basis sets.

	D: $1s2s^2\ ^2S$		E: $1s[2s2p\ ^3P]^2P$		F: $1s[2s2p\ ^1P]^2P$		G: $1s2p^2\ ^2D$		H: $1s2p^2\ ^2S$	
Result	Energy	Width	Energy	Width	Energy	Width	Energy	Width	Energy	Width
[a]	410.629	77.90	421.176	9.4	426.206	43.2	429.102	57.64	437.58	14.33
Expt.[b]			421.47 ± 0.03	11 ± 8	425.45 ± 0.03					
RM[b]			421.448	4	425.606	42				
MCDF[b]			421.390		425.654					
[c]	410.156	64.55	420.225	9.8	425.312	31.08	429.243	71.0	437.187	11.05
[d]	409.465	55.62	420.876	6	425.639	40.01	429.428	69.55	437.629	13.14
[e]	410.900	86.0	421.169	6.42						
[f]			421.049	4.2	425.329	41.63				
[g]			421.605	5.88	...	42.68				

[a]Present work.
[b]Experiment and theory (R-matrix and MCDF), Shorman *et al.*[2]
[c]MCDF, Chen and Crasemann.[4,6]
[d]R-matrix, Garcia *et al.*[10]
[e]C-MRCI, Zhang and Yeager.[12]
[f]SPCR, Davis and Chung.[14]
[g]SPCR, Wu and Xi.[15]

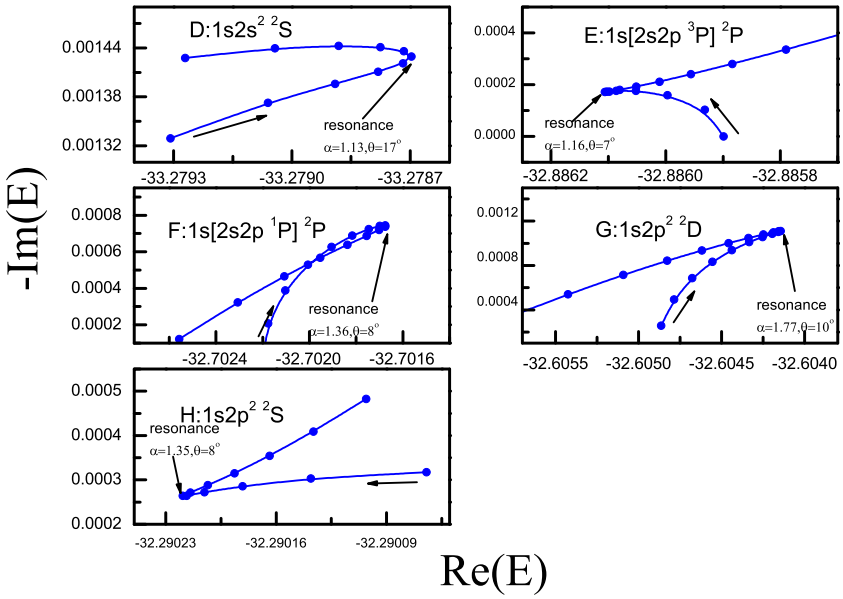

FIG. 2. θ trajectory for Auger states D–H of N^{4+}, α are 1.13, 1.16, 1.36, 1.77, and 1.35, respectively. The step length is 1°. The calculated ground energy of N^{4+} ($1s^2 2s\ ^2S$) is −48.3706 a.u. and −48.3714 a.u. with basis sets 14s8p and 14s8p4d, respectively.

and the theoretical calculations have been performed by R-matrix,[2,10] MCDF,[2,4,6] CMR-CI,[12] and saddle-point complex rotation (SPCR).[15,16] Excellent agreement is found between the measured data and the present calculations; the resonance position differences are 0.29 eV and 0.75 eV for states E and F (the relative differences are less than 0.2%), respectively. Note that the present calculated Auger width of state E is 9.4 meV, which is very close to 9.8 meV of MCDF[4,6] but differs a lot from 4 meV to 6 meV of R-matrix,[10] CMR-CI[12] and SPCR;[15,16] however, the experimental result is 11 ± 8 meV, the error bar is too big to finally determine the Auger decay width, and more precise measurements are required in the future. For other states D, G, and H, relatively good agreements are achieved between the present calculations and other available calculations.[2,4,6,10,12,15,16]

Table V shows the resonance parameters of I, J, K, L, M, N, O, and P of N^{3+}. The last θ-trajectories and the resonances are presented in Fig. 3. There are experimental data for

TABLE V. Auger resonance positions (eV) and widths (meV) of N^{3+} ion relative to the ground state $1s^2 2s^2\ ^1S$ of N^{3+} with the same basis sets.

	I: $1s2s^2 2p\ ^1P$		J: $1s2s^2 2p\ ^3P$		K: $1s[2s2p^2\ ^4P]^3P$		L: $1s[2s2p^2\ ^2P]^3P$	
Result	Energy	Width	Energy	Width	Energy	Width	Energy	Width
[a]	414.71	66.37	410.79	76.26	420.280	10.57	426.206	67.26
Expt.[b]	414.03 ± 0.03	93 ± 13			420.74 ± 0.03	85 ± 14		
R-matrix[b]	414.043	60			420.698	12		
MCDF[b]	414.104	...			419.265	...		
[c]	412.590	54.94	408.95	77.73	418.459	25.54	425.480	58.81
[d]	413.872	49.43	410.100	72.47	420.355	13.17	428.505	55.57
[e]	412.275	65.3	408.644	96.3			427.575	55.0
[f]	413.197	57.96	410.230	79.0	420.715	10.8		
	M: $1s2s2p^2\ ^3D$		N: $1s2s2p^2\ ^1S$		O: $1s2s2p^2\ ^1P$		P: $1s2s2p^2\ ^1D$	
Result	Energy	Width	Energy	Width	Energy	Width	Energy	Width
[a]	420.550	40.39	430.741	85.54	432.177	26.3	427.496	127.73
Expt.[b]	421.23 ± 0.03	46 ± 32						
RM[b]	420.861	59						
MCDF[b]	419.414							
[c]	419.583	53.94	429.858	94.75	429.859	13.21	425.379	129.56
[d]	421.096	63.10	431.726	78.92	431.161	16.95	427.117	115.72
[f]	420.824	57.7						

[a]Present work.
[b]Experiment and theory (R-matrix and MCDF), Shorman *et al.*[2]
[c]MCDF, Chen and Crasemann.[5,7]
[d]R-matrix, Garcia *et al.*[10]
[e]C-MRCI, Zhang and Yeager.[13]
[f]SPCR, Lin *et al.*[18,19]

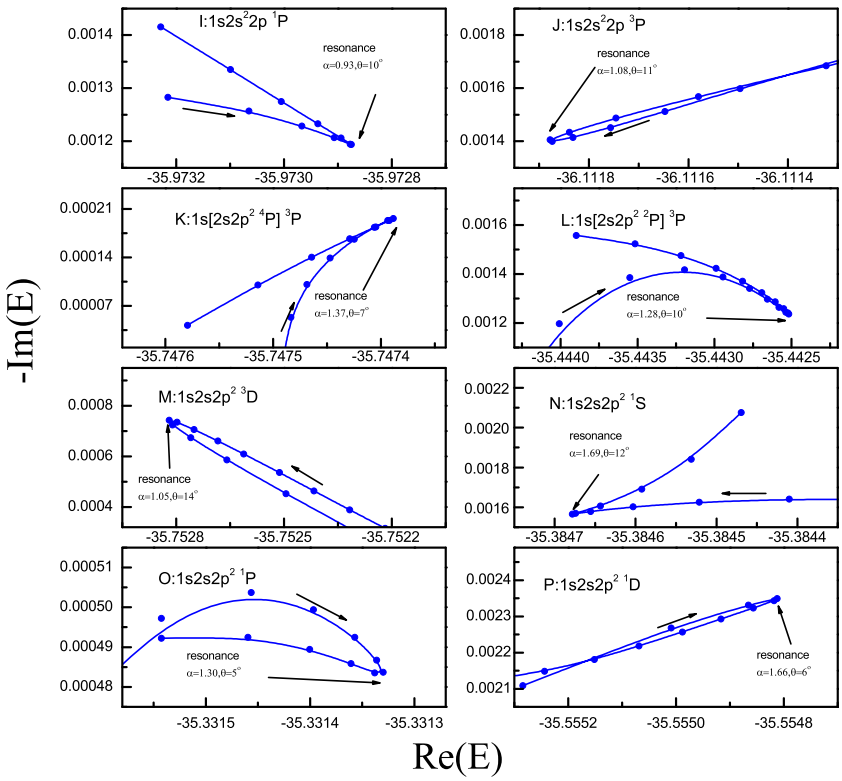

FIG. 3. θ trajectory for Auger states I–P of N^{3+}, α are 0.93, 1.08, 1.37, 1.28, 1.05, 1.69, 1.30, and 1.66, respectively. The step length is 1°. The calculated ground energy of N^{3+} ($1s^2 2s^2\ ^1S$) is −51.2134 a.u. and -51.2157 a.u. with basis sets 14s8p and 14s8p4d, respectively.

TABLE VI. Auger resonance positions (eV) and widths (meV) of N^{2+} ion relative to the ground state $1s^2 2s^2 2p\ ^2P$ of N^{2+} with the same basis sets.

	Q: $1s2s2p^3\ ^4D$		R: $1s2s2p^3\ ^4P$		S: $1s[2s2p^3\ ^5S]\ ^4S$		T: $1s2s^22p^2\ ^2D$	
Result	Energy	Width	Energy	Width	Energy	Width	Energy	Width
[a]	411.618	69.20	414.347	47.58	411.014	17.71	406.41	110.47
Expt.[b]	411.88 ± 0.03	36 ± 19					405.81 ± 0.03	122 ± 19
RM[b]	411.866	62	414.664	48	412.224	15	405.703	122
MDCF[b]	411.874		415.633		412.860		405.890	
SCUNC[b]	412.020	56	414.670	15	412.600	11	405.980	123
[c]	412.780	63.07	415.518	48.99	410.104	26.85	404.826	109.67
[d]	412.121	68.22	414.840	51.24	411.188	18.10	405.965	109.09
	U: $1s2s^22p^2\ ^2P$		V: $1s2s^22p^2\ ^2S$		W: $1s[2s2p^3\ ^3S]\ ^4S$		X: $1s[2s2p^3\ ^3S]\ ^2S$	
Result	Energy	Width	Energy	Width	Energy	Width	Energy	Width
[a]	407.007	64.0	408.197	118.6	422.389	69.62	426.446	19.74
Expt.[b]	406.55 ± 0.03	58 ± 7	408.38 ± 0.03	120 ± 60				
RM[b]	406.656	62	408.344	106				
MCDF[b]	406.380	…	410.085	…				
SCUNC[b]	406.561	66	408.414	132				
[c]	406.702	51.47	406.767	101.10	422.370	72.47	427.078	24.17
[d]	406.387	44.48	408.297	94.68	422.656	62.14	426.243	24.54
	Y: $1s[2s2p^3\ ^3P]\ ^2P$		Z: $1s[2s2p^3\ ^1P]\ ^2P$		Z′: $1s[2s2p^3\ ^3D]\ ^2D$		Z″: $1s[2s2p^3\ ^1D]\ ^2D$	
Result	Energy	Width	Energy	Width	Energy	Width	Energy	Width
[a]	420.22	73.21	424.62	85.51	421.709	103.83	417.463	92.96
[c]	419.584	87.16	425.773	95.93	423.033	114.96	417.554	101.63
[d]	421.067	78.95	426.182	94,79	423.439	111.76	418.345	98.01

[a]Present work.
[b]Experiment and theory (R-matrix, MCDF, and SCUNC), Gharaibeh *et al.*[3]
[c]MCDF, Chen and Crasemann.[5,7]
[d]R-matrix, Garcia *et al.*[10]

states I, K, and M, which are measured by Gharaibeh *et al.*[2] on the SOLEIL synchrotron radiation facility. As shown in Table V, for states I and M, there are fairly good agreements on both the resonance positions and widths between the present calculations and the measurements,[2] as well as other calculations.[2,5,7,10,13] For state K, all the calculations predict the Auger width in the range of 10 meV–20 meV; however, the measured data are 85 ± 14 meV.[2] State M is only 0.5 eV above state K, their close overlapping increases the measurement difficulties.[2] Further theoretical and experimental studies need to be performed to finally determine the Auger width. There are no experimental data for the remaining five resonance states J, L, N, O, and P of N^{3+}. Table V shows that the present calculations for those five states agree well with the other calculations.[2,5,7,10,13] But the present width of state O is larger than the prediction of MCDF[5,7] and R-matrix.[10]

The resonance parameters for the 12 Auger states of N^{2+} ions are presented in Table. VI, while the last θ-trajectories and the resonances are presented in Fig. 4. As shown in the table, for states Q, T, U, and V, the present CMRD-CI calculations are in excellent agreement with the available SOLEIL measurements,[3] as well as other calculations.[3,8–10] For the other eight states R, S, W, X, Y, Z, Z′, and Z″, very good agreements are achieved for different calculations.[3,8–10]

It is interesting to show the spin-alignment phenomenon[59,60] in the present calculations of K-vacancy Auger states, namely, the Auger decay rate or Auger width depends on the spin-alignment for the pair KL_1L_2 states with different multiplicities (e.g., states $1s[2s2p\ ^1P]\ ^2P$ and $1s[2s2p\ ^3P]\ ^2P$). As proposed by Chung *et al.*,[59,60] the Auger decay process is more likely to occur when the two reaction electrons have strong interactions: KL_1L_1 states decay faster than KL_1L_2 states, and in the case of KL_1L_2 states, the decay is faster if the L_1 and L_2 electrons have opposite spin. The spin-alignment rule can help us to qualitatively understand the changes of the resonance widths for some Auger states.

For states N^{5+} $(2s^2)$ and N^{5+} $(2s2p)$, it is obvious that the two 2s electrons overlap more than the 2s and 2p electrons and the interactions of the two 2s electrons are stronger than the 2s and 2p electrons, the decay width of the former state should be larger than the latter one, which is consistent with the results shown in Table III. For states B $[N^{5+}\ (2s2p\ ^1P)]$ and C $[N^{5+}\ (2s2p\ ^3P)]$, the calculations show that the former one decays faster. According to the spin-alignment rule, the interactions between the 2s and 2p electrons are expected to be stronger for the former state; as shown in Fig. 5, the overlaps of the radical wavefunction for the singlet state are larger than that of the triplet one. Similarly, this simple rule can be applied to understand other states such as E and F, K and L, and S and W. However, the conditions become more complex for states Y and Z and Z′ and Z″, the simple qualitatively rule does not work any more.

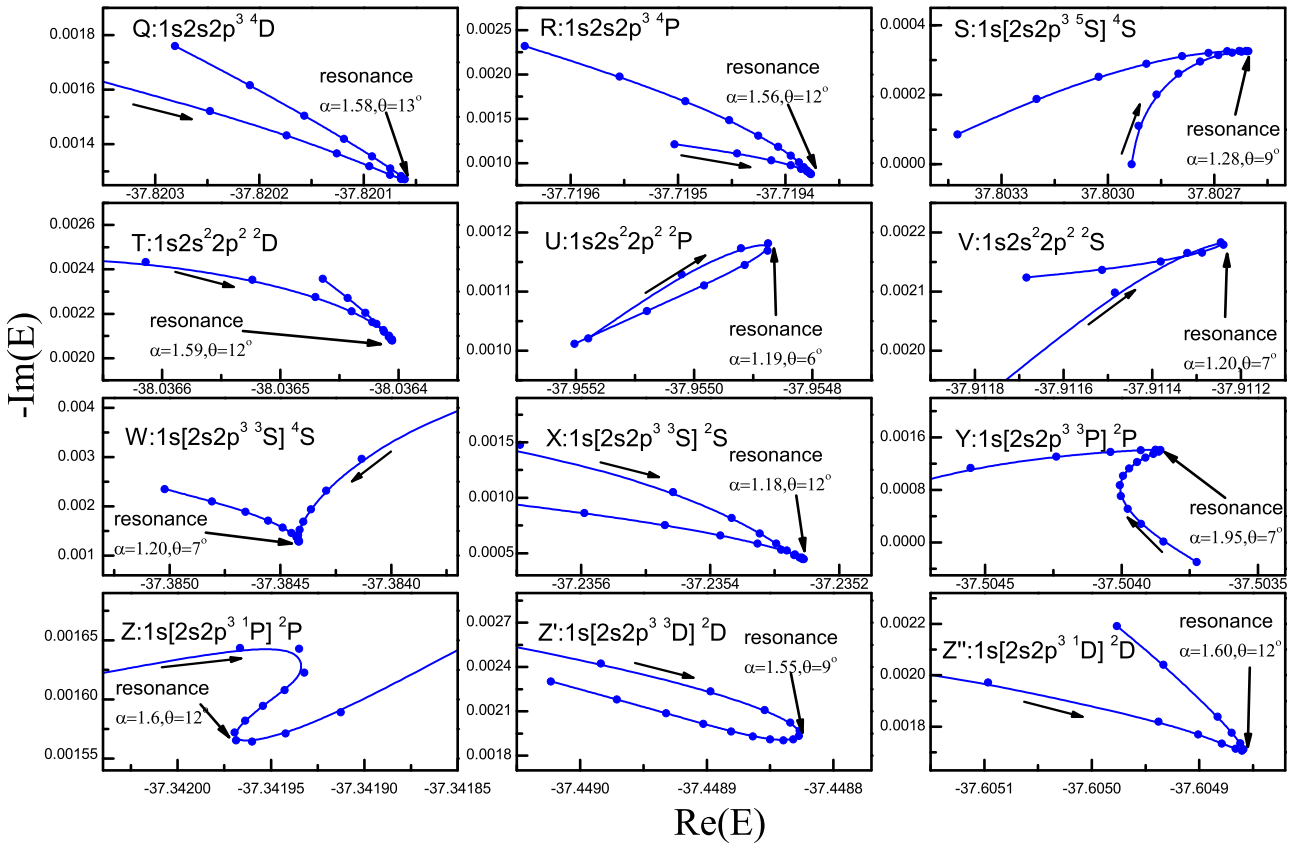

FIG. 4. θ trajectory for Auger states Q–Z″ of N^{2+}, α are 1.58, 1.56, 1.28, 1.59, 1.19, 1.20, 1.20, 1.18, 1.95, 1.60, 1.55, and 1.60, respectively. The step length is 1°. The calculated ground energy of N^{2+} $(1s^22s^22p\ ^2P)$ is −52.9314 a.u. and −52.9446 a.u. with basis sets 14s8p and 14s8p4d, respectively.

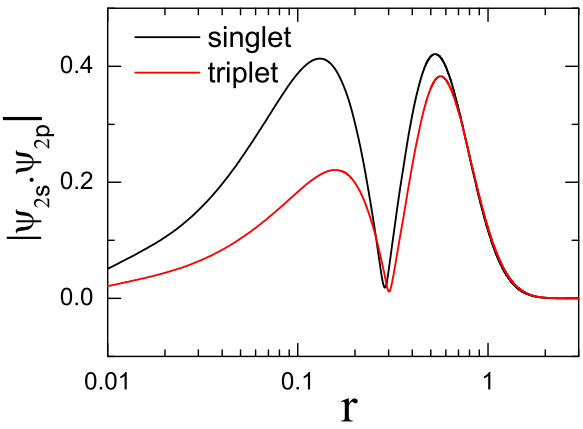

FIG. 5. The product of the radial orbital wavefunction $|\psi_{2s}\cdot\psi_{2p}|$ for singlet and triplet states.

IV. SUMMARY

The CMRD-CI method is first employed to study the K-vacancy Auger states of N^{q+} (q = 2-5) ions. Accurate resonance parameters are obtained. Within the framework of the complex scaling method, the Auger resonance state can be studied as a bound state and described well by a small Gaussian basis set. It is significant to fully consider the strong correlations between the core and valence electrons in the calculations, while the Rydberg electrons do not play important roles. The spin-alignment rule can be applied to qualitatively understand the changes of the Auger decay rates. The calculated resonance parameters are in excellent agreement with the available experimental and theoretical data. However, further experimental studies are needed to determine the resonance parameters and check the calculations.

In the present study, full CI calculations are performed based on the complex basis sets modified from cc-pv5z of nitrogen. With respect to the energy uncertainty, there are mainly two types of possible error sources. One arises from the finite basis set applied in the calculation and the other is from the non-relativistic treatment of eigenvalues of the Schrödinger equation. The truncation errors of the basis sets can be estimated with increase of the size of the basis set, as examples shown for the states $1s2s^2\,{}^2S$ and $1s[2s2p\,{}^3P]\,{}^2P$ of N^{4+} in Table II. It can be observed that the absolute energy errors are about 10^{-3} a.u. and 2×10^{-4} a.u., approximately 0.003% and 6.7%, for the resonance position and widths for the state $1s2s^2\,{}^2S$; and the errors are about 3×10^{-4} a.u. and 9×10^{-5} a.u., approximately 0.001% and 30%, for the resonance position and widths for the state 1s $[2s2p\,{}^3P]\,{}^2P$. The relativistic effects for low nuclear charge Z atomic energy can be estimated well by using the perturbation theory, and the dominant relativistic correction is of relative order $Z^2\alpha^2$, which is about 0.26% for nitrogen and α is the fine-structure constant. Combining the above error contributions from the basis set truncation and the relativistic correction, the resonance position uncertainties are estimated with order of 0.3%, and the error of resonance widths amounts to 10^{-5}–10^{-4} a.u. dependent on the width value, with uncertainty of 7% for the widths with order 10^{-3} a.u. and 30% for the case of 10^{-4} a.u. widths.

The present CMRD-CI method can serve as an efficient tool in treating the atomic K-vacancy resonance states and the double-electron recombination process in electron-atom collisions. Moreover, the present CMRD-CI method is directly applicable to molecular resonance states, including the auto-ionization and dissociative states, which are necessary parameters in studying the dynamics processes of molecules, for example, interatomic Coulomb decay processes.

ACKNOWLEDGMENTS

This work was supported by the National Basic Research program of China under Grant No. 2013CB922200 and the National Natural Science Foundation of China under Grant Nos. 11474032, 11474033, and U1332204. We thank Dr. M. Honigmann for helpful discussions on the use of the CMRD-CI code.

[1]M. A. Leutenegger, S. M. Kahn, and G. Ramsay, Astrophys. J. **585**, 1015 (2003).
[2]M. M. A. Shorman, M. F. Gharaibeh, J. M. Bizau, D. Cubaynes, S. Guilbaud, N. E. Hassan, C. Miron, C. Nicolas, E. Robert, I. Sakho *et al.*, J. Phys. B: At., Mol. Opt. Phys. **46**, 195701 (2013).
[3]M. F. Gharaibeh, N. E. Hassan, M. M. A. Shorman, J. M. Bizau, D. Cubaynes, S. Guilbaud, I. Sakho, C. Blancard, and B. M. McLaughlin, J. Phys. B: At., Mol. Opt. Phys. **47**, 065201 (2014).
[4]M. H. Chen, B. Crasemann, and H. Mark, Phys. Rev. A **27**, 544 (1983).
[5]M. H. Chen, Phys. Rev. A **31**, 1449 (1985).
[6]M. H. Chen, At. Data Nucl. Data Tables **34**, 301 (1986).
[7]M. H. Chen and B. Crasemann, At. Data Nucl. Data Tables **37**, 419 (1987).
[8]M. H. Chen and B. Crasemann, Phys. Rev. A **35**, 4579 (1987).
[9]M. H. Chen and B. Crasemann, At. Data Nucl. Data Tables **38**, 381 (1988).
[10]J. Garcia, T. R. Kallman, M. Witthoeft, E. Behar, C. Mendoza, P. Palmeri, P. Quinet, M. Bautista, and M. Klapisch, Astrophys. J., Suppl. Ser. **185**, 477 (2009).
[11]J. Hata and I. P. Grant, J. Phys. B: At. Mol. Phys. **16**, L125 (1983).
[12]S. B. Zhang and D. L. Yeager, J. Mol. Struct. **1023**, 96 (2012).
[13]S. B. Zhang and D. L. Yeager, Phys. Rev. A **85**, 032515 (2012).
[14]B. F. Davis and K. T. Chung, Phys. Rev. A **39**, 3942 (1989).
[15]L. Wu and J. Xi, J. Phys. B: At., Mol. Opt. Phys. **24**, 3351 (1991).
[16]K. T. Chung, Phys. Rev. A **42**, 645 (1990).
[17]W. C. Shiu, C.-S. Hsue, and K. T. Chung, Phys. Rev. A **64**, 022714 (2001).
[18]S.-H. Lin, C.-S. Hsue, and K. T. Chung, Phys. Rev. A **64**, 012709 (2001).
[19]H. Lin, C.-S. Hsue, and K. T. Chung, Phys. Rev. A **65**, 032706 (2002).
[20]H. Y. Yang and K. T. Chung, Phys. Rev. A **51**, 3621 (1995).
[21]F. Wang and B. Gou, At. Data Nucl. Data Tables **92**, 176 (2006).
[22]Y. Gning, M. Sow, A. Traoré, M. Dieng, B. Diakhate, M. Biaye, and A. Wagué, Radiat. Phys. Chem. **106**, 1 (2015).
[23]Y. K. Ho, J. Phys. B: At., Mol. Opt. Phys. **12**, 387 (1979).
[24]Y. Ho, Phys. Lett. A **79**, 44 (1980).
[25]Y. K. Ho, Phys. Rev. A **23**, 2137 (1981).
[26]G. W. F. Drake and A. Dalgarno, Proc. R. Soc. A **320**, 549 (1971).
[27]J. M. Seminario and F. C. Sanders, Phys. Rev. A **42**, 2562 (1990).
[28]M. Biaye, A. Kont, A. S. Ndao, N. A. B. Faye, and A. Wagu, Phys. Scr. **71**, 39 (2005).
[29]M. Biaye, A. Konte, A. S. Ndao, and A. Wague, Phys. Scr. **72**, 373 (2005).
[30]I. Sakho, A. S. Ndao, M. Biaye, and A. Wague, Eur. Phys. J. D **47**, 37 (2008).
[31]A. Konta, A. S. Ndao, M. Biaye, and A. Wague, Phys. Scr. **74**, 605 (2006).
[32]L. W. Manning and F. C. Sanders, Phys. Rev. A **44**, 7206 (1991).
[33]L. Lipsky, R. Anania, and M. Conneely, At. Data Nucl. Data Tables **20**, 127 (1977).
[34]A. Derevianko, V. A. Dzuba, and M. G. Kozlov, Phys. Rev. A **82**, 022720 (2010).
[35]R. J. Buenker, in *Proceedings of the Workshop on Quantum Chemistry and Molecular Physics* (University of Wollongong Press, Wollongong, Australia, 1980).
[36]R. J. Buenker, *Current Aspects of Quantum Chemistry* (Elsevier, Amsterdam, 1982), Vol. 21.
[37]R. J. Buenker and R. A. Phillips, J. Mol. Struct. **123**, 291 (1985).
[38]R. Buenker, Russ. J. Phys. Chem. B **8**, 14 (2014).

[39]R. J. Buenker and S. D. Peyerimhoff, Theor. Chim. Acta **35**, 33 (1974).
[40]M. Honigmann, Ph.D. thesis, Universitat Wuppertal, 1989.
[41]D. B. Knowles, J. R. Alvarez Collado, G. Hirsch, and R. J. Buenker, J. Chem. Phys. **92**, 585 (1990).
[42]S. B. Zhang and D. L. Yeager, Mol. Phys. **110**, 663 (2012).
[43]S. B. Zhang and D. L. Yeager, Phys. Rev. A **85**, 054502 (2012).
[44]J. Aguilar and J. Combes, Commun. Math. Phys. **22**, 269 (1971).
[45]E. Balslev and J. Combes, Commun. Math. Phys. **22**, 280 (1971).
[46]B. Simon, Commun. Math. Phys. **27**, 1 (1972).
[47]W. P. Reihardt, Annu. Rev. Phys. Chem. **33**, 223 (1982).
[48]C. W. McCurdy, Phys. Rev. A **21**, 464 (1980).
[49]C. W. McCurdy, T. N. Rescigno, E. R. Davison, and J. Lauderdale, J. Chem. Phys. **73**, 3268 (1980).
[50]T. N. Rescigno, C. W. McCurdy, and A. E. Orel, Phys. Rev. A **17**, 1931 (1978).
[51]M. Honigmann, R. J. Buenker, and H.-P. Liebermann, J. Chem. Phys. **125**, 234304 (2006).
[52]M. Honigmann, R. J. Buenker, and H.-P. Liebermann, J. Chem. Phys. **131**, 034303 (2009).
[53]M. Honigmann, H.-P. Liebermann, and R. J. Buenker, J. Chem. Phys. **133**, 044305 (2010).
[54]M. Honigmann, G. Hirsch, R. J. Buenker, I. D. Petsalakis, and G. Theoorakopoulos, Chem. Phys. Lett. **305**, 465 (1999).
[55]E. R. Davison, Comput. Phys. **7**, 519 (1993).
[56]M. Hanrath and B. Engels, Chem. Phys. **225**, 197 (1997).
[57]T. H. Dunning, J. Chem. Phys. **90**, 1007 (1989).
[58]N. Moiseyev, S. Friedland, and P. R. Certain, J. Chem. Phys. **74**, 4739 (1981).
[59]K. T. Chung, Phys. Rev. A **59**, 2065 (1999).
[60]K. T. Chung and B. F. Davis, *Autoionization: Recent Development and Applications* (Plenum, New York, 1985).